INDIAN JOURNAL OF
ENGINEERING

18(49), 2021

Investigating the lumped-heat-capacity assumption of thermal analysis in fibre mat composites

Cornelius Ogbodo Anayo Agbo✉

To Cite:
Agbo COA. Investigating the lumped-heat-capacity assumption of thermal analysis in fibre mat composites. *Indian Journal of Engineering*, 2021, 18(49), 172-184

Author Affiliation:
Department of Mechanical Engineering, University of Nigeria, Nsukka, Nigeria

✉**Corresponding author:**
Cornelius Ogbodo Anayo Agbo,
Department of Mechanical Engineering, University of Nigeria, Nsukka, Nigeria
Email: cornelius.agbo@unn.edu.ng

Peer-Review History
Received: 13 April 2021
Reviewed & Revised: 16/April/2021 to 07/May/2021
Accepted: 09 May 2021
Published: May 2021

Peer-Review Model
External peer-review was done through double-blind method.

DISCOVERY
SCIENTIFIC SOCIETY

ABSTRACT

The temperature gradient through the thickness of a composite material contributes to the thermal stresses experienced by the finally cured laminate. This paper seeks to evaluate the appropriate laminate thickness range where lumped-heat-capacity analysis can be applied. The conditions as evaluated made use of the Biot parameter. The material's conductivity and the surface convection heat transfer coefficient coupled with the environmental conditions determine the borderline thickness for either using the lumped capacity analysis or the more detailed analysis. The variations in these parameters determine the temperature gradient through the thickness of the material. A numerical analysis carried out was validated using experimental tests. The results showed a negligible difference. The lumped-heat capacity assumption is therefore suitable in fibre mat composite analysis.

Keywords: polymer composites, lumped-capacity, thermal properties, Biot parameter, thermal analysis

1. INTRODUCTION

The existence of spatial change in temperature in materials ensures that heat is conducted from one point to another within the material and the exchange of heat with the ambient. The temperature distribution in a laminate during cure influences the resultant residual stresses in the component and therefore require careful investigation and control. The temperature distribution in the laminate would depend on the material's thermal conductivity and the heat-transfer conditions from the laminate surface to the surrounding fluid. Reasonably uniform temperature distribution in the laminate would occur if the resistance to heat transfer by conduction were very small compared to the convection resistance at the surface so that the major temperature gradient would occur through the fluid layer at the surface. The lumped-heat-capacity analysis, then, assumes that the magnitude of the material's external resistance is very much greater than the material's internal resistance (Holman, 2001). Composite structures exhibit inherent processing defects some of which can be detrimental to the mechanical performance or constitute a nuisance than a significant problem; these defects include voids, delamination, residual stress-induced cracking, resin starvation, resin-rich pockets, damaged fibres, fibre-matrix debonding, thermal decomposition, and under cured and over cured

regions. The temperature field inside the fibre composite is very complex and directly affects the fusion quality between plies. There exists a characteristic nonlinear process in the internal temperature of the matrix as its temperature is raised during cure at it affects the quality of bonding of the composite layers and the component products (Cao et al., 2020). A major problem that could arise from the application of composite laminates is perhaps that of cracking due to large temperature differentials.

Polymer composites generally are processed at increased temperatures, while thermoset matrix materials require elevated temperatures to cure, and thermoplastic matrix materials require elevated temperatures for the melting required for consolidation of layers. After a while at the elevated temperature state, the composite temperature is reduced, eventually reaching ambient temperature. Though the composite is soft and stress-free at the elevated temperature, at some point in the cooling process the material hardens to the point that the elastic and thermal expansion properties of the composite are identifiable. As the temperature of the composite goes below thermally induced stresses begin to develop (Hyer, 1998). Ultimately when the glassy state is reached, there remains a significant state of permanent stress, the residual stress state (Christensen, 1982). In the general case of heat flow, the temperature is not a straight-line function of the dimensions of a body. Since each element of a body is constrained by the other elements, it is not free to expand, and consequently, if the temperature gradient is not linear, internal stress will develop. Residual stresses are a system of stresses which can exist in a body when it is free from external forces and are generated by nonuniform plastic deformation (Dieter, 1988). The temperature gradient is likely to increase with the thickness of the laminate; therefore, greater thermal stress can be expected in thick laminates than in thin ones as the stress is directly proportional to the linear coefficient of thermal expansion, to the difference in temperature at the two faces of the laminate, and the modulus of elasticity (Agbo, 2016).

After the cure cycle, deformations encountered during cure due to chemical and thermal changes coupled with the mould constraint are balanced internally in the component which results in residual stress that can cause low performance through warpage, shape distortions, matrix cracks and delamination within the manufactured part. An optimization process to predict accurately and measure accruing residual stresses and strain developments during the cure cycle constitute important issues needed to be addressed (Antonucci, 2006).

Many polymeric composite laminates, like graphite/epoxy, undergo a substantial temperature change as they cool down after cure. The thermal excursions induce significant residual stress into the composite laminate because of the thermal expansion mismatch between the fibre and the matrix. The residual stress dependence on temperature history is attributable to two contradictory roles of temperature. While at elevated temperature stress relaxation occurs, upon cooling against geometric constraints, temperature acts as a stress-inducing agent (Weitsman, 1979). Linear elastic stress analysis predicts that the thermal stress, which develops within a composite material due to typical temperature excursions undergone by the structure, may exhaust the strength in various laminae even before external loads are applied (Lee and Weitsman, 1994). A major proportion of the thermal stresses is developed in the composite during cooling from cure temperature down to room temperature. This cool down stage can be considered as a part of the component manufacturing sequence and therefore lends itself to careful control. The cool-down path details appear to influence the magnitude of the residual stresses more noticeably than the duration of the cooling period. Thermal excursions induce significant residual thermal stress in composite laminate structures as an unavoidable problem of the large difference in the thermal expansion coefficient of the reinforcement fibres and the polymeric matrix. The presence of temperature gradient across the laminate thickness during cooling contributes to the development of residual stress in composites. This is due to the thermo-mechanical properties of the composites on temperature. As different sections of the composite laminate experience varying temperature histories, the deformations accruing therefrom will also differ. An inconsistency in the deformation response occurring in the laminate naturally leads to the development of residual stresses. Residual stresses may cause significant damages in composite structures, through void formation or fibre buckling during solidification, initiation of transverse cracks and delamination which reduces strength with a deleterious consequence on the component performance (Sonmez, 2002).

In many studies done by earlier researchers, the temperature was assumed to be uniform across the plate thickness at any given time and so neglecting the effects of temperature gradient induced during cooling (Sonmez, 2002). Li et al. (2013) developed a model based on finite element analysis to predict residual stress occurring in thermoplastic composites. The values obtained indicated that both the sequence of the laminate layup and the distribution of crystallinity are affected differently by the cooling rate. Certain minimization of residual stress due to cure may result by understanding the cool-down path after cure. Although the residual stresses reduction in composites is not dramatic, they serve to indicate that additional benefits may accrue if a more scientific approach is taken toward the entire production cure process (Kibler, 1980). This paper, therefore, hoped to work towards predicting better temperature distribution criteria for a reduced residual thermal stress analysis.

ISSN 2319–7757 EISSN 2319–7765 | OPEN ACCESS

2. THERMAL RESPONSE ANALYSIS

Even though lumped heat capacity systems are considered uniform in temperature, these are idealized condition because a temperature gradient must exist within the material if heat can be conducted into or out of the body, in cooling a material within an environment, the spatial temperature distribution in the material would depend on the material's thermal conductivity and the overall heat transfer conditions from the surface. A reasonably uniform temperature distribution exists when the resistance to conduction heat transfer was small compared to the convection heat transfer resistance from the surface so that the major temperature gradient would occur across the fluid layer at the surface. The lumped heat capacity analysis, therefore, presumes the internal conductive resistance of material negligible compared to external convective resistance. In that case, the convection heat loss from the body is evidenced by a decrease in the internal energy of the body (Holman, 2001). The classical lumped parameter analysis applies to various thermal engineering systems with low to moderate temperature gradient where the evaluated Biot number is below 0.1 (An and Su, 2015). A developed model of lumped capacitance was shown as a good replacement to the computationally complex CFD model in predicting the phenomenon associated with the transients in heat transfer (Tegenaw et al., 2019).

Heat Transfer Cooling Analysis

Transient cooling analysis of the heat transfer is required to obtain the temperature distribution within the laminate and the temperature gradient through the laminate thickness during cooling. Necessary assumptions and boundary conditions were made to enable feasible diagnostics. The in-plane dimensions of the laminate were assumed to be very large compared to the thickness. Consequently, heat transfer through the edges has been neglected in comparison to the top or bottom surfaces of the laminate. The in-plane temperature distribution is accordingly assumed to be uniform. Thermal analysis of one-dimensional heat transfer is, therefore, considered and expected to yield acceptable results.

The laminate's upper surface is cooled by the convective heat transfer by the surrounding air, while the lower surface in contact with the mould is cooled by conduction heat transfer across the galvanized steel mould (see Fig. 1). The mould is in turn cooled by convection through the surrounding air. The conduction through the air film and radiation are all lumped into the convective overall heat transfer. The steel mould thickness is thin and highly conductive compared to composite laminate, hence the temperature at the laminate bottom is assumed to be the same as at the mould bottom.

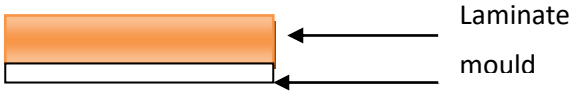

Fig. 1 Laminate in mould undergoing cure process

To establish an empirical value for the coefficient of heat transfer to be used, Nusselt number is sought as follows;

The top surface of heated laminate as given by McAdams (1954):

$$\overline{Nu}_f = 0.54(Ra)^{1/4} \quad \text{if} \quad 10^4 < Gr_f . Pr_f < 10^7$$

$$= 0.15(Ra)^{1/3} \quad \text{if} \quad 10^7 < Gr_f . Pr_f < 10^{11} \qquad (1)$$

The bottom surface of heated laminate as given by McAdams (1954):

$$\overline{Nu}_f = 0.27(Ra)^{1/4} \quad \text{if} \quad 10^5 < Gr_f . Pr_f < 10^{10} \qquad (2)$$

Where Nu = Nusselt number

$Gr = g\beta L^3 \Delta T/\nu^2 =$ Grashof number

$P_r = \frac{\nu}{\alpha}$ = Prandtl number

ISSN 2319–7757 EISSN 2319–7765 | OPEN ACCESS

Ra = Raleigh number = Gr . Pr

g = acceleration of gravity, ν = kinematic viscosity, α = thermal diffusivity, β = 1/T is the volume coefficient of expansion, ΔT = temperature difference between the wall and the ambient, L= characteristic dimension, ϱ = density, τ = time constant,

The fluid properties are determined at the mean film temperature,

$T_f = \frac{(T_0+T_\infty)}{2}$ where f indicates evaluation at film conditions

Simplified equations for the heat transfer coefficients from surfaces to surrounding air at atmospheric pressure and moderate temperatures can also be approximated as follows (Holman, 2001):

heated laminate facing upward, $h = 1.32(\Delta T/L)^{1/4}$ laminar flow $10^4 < Gr_f Pr_f < 10^9$

$h = 1.52(\Delta T)^{1/3}$ turbulent flow $Gr_f Pr_f > 10^9$

heated laminate facing downward $h = 0.59(\Delta T/L)^{1/4}$ both turbulent and laminar

where h= heat transfer coefficient W/m²K

$\Delta T = T_w - T_\infty$, ℃

L = vertical or horizontal dimension, m

The laminate was kept horizontal on the mould to avoid resin overflow and/or work sliding down. The governing heat balance equation is stated thus:

$$q = hA(T - T_\infty) = -c\rho V dT/dt$$

where A is surface area, V = volume

The initial condition

$T = T_0$ at time t = 0

So that the solution gives

$$\frac{(T - T_\infty)}{(T_0 - T_\infty)} = e^{-(hA/\rho CV)t}$$

Where T∞ is the temperature of the surrounding

This analysis is expected to yield reasonable estimates within about 5% when the following condition is met.

$$h(V/A)/k < 0.1$$

where k = thermal conductivity.

The dimensionless group is known as

Biot number = $hs/k = Bi$

S = V/A is a characteristic length dimension.

ISSN 2319–7757 EISSN 2319–7765 I OPEN ACCESS

A representative element is shown in Fig. 2 to analyse the process of heat transfer within the composite. The Fouriers equation is established within the principle of the heat balance.

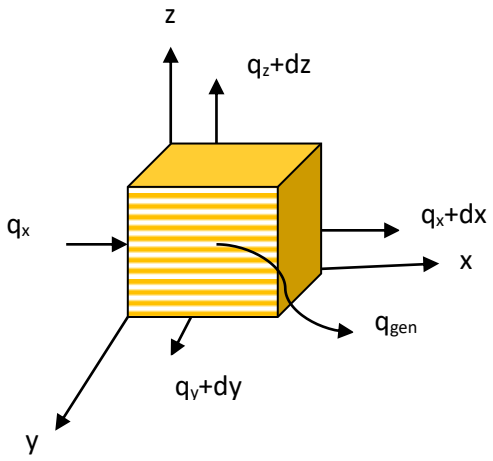

Fig. 2 Heat transfer element from a laminate

$$q = -kA\frac{dT}{dz} \qquad (3)$$

Nevertheless, the general three- dimensional heat conduction equation is

$$\frac{\partial^2 T}{\partial x^2} + \frac{\partial^2 T}{\partial y^2} + \frac{\partial^2 T}{\partial z^2} + \frac{\dot{q}}{k} = \frac{1}{\alpha}\frac{\partial T}{\partial t} \qquad (4)$$

where the quantity $\alpha = \frac{k}{\rho c}$ is called the thermal diffusivity of the laminate.

For the one-dimensional case with constant properties, the differential equation for the temperature distribution $T(z,t)$ in equation (4) is reduced to

$$\frac{\partial^2 T}{\partial z^2} = \frac{1}{\alpha}\frac{\partial T}{\partial t} \qquad (5)$$

the initial condition is $T(z,0) = T_i$

the convection boundary condition

$hA(T_\infty - T)_{z=0} = -kA\frac{\partial T}{\partial z}$ at $z = 0$

The explicit forward difference equations are employed to predict the temperature distribution in the laminate as a discrete function of space and time.

For the internal nodes, we have

ISSN 2319–7757 EISSN 2319–7765 | OPEN ACCESS

$$T_m^{p+1} = \frac{\alpha \Delta t}{(\Delta z)^2}\left(T_{m+1}^p + T_{m-1}^p\right) + \left[1 - \frac{2\alpha \Delta t}{(\Delta z)^2}\right] T_m^p \qquad (6)$$

and if the time and distance increments are chosen so that $\frac{(\Delta z)^2}{\alpha \Delta t} \geq 2$, stability is ensured.

The temperature of node m after the time increment is given as the arithmetic average of the two adjacent nodal temperatures at the beginning of the time increment.

This restriction automatically limits our choice of Δt, once Δz is established.

On the convective surface of the composite laminate, the total energy conducted and convected into the node equals the increase in the internal energy at the node. Thus

$$k \Delta y \frac{T_{m-1}^p - T_m^p}{\Delta z} + h \Delta y \left(T_\infty - T_m^p\right) = \rho c \frac{\Delta z}{2} \Delta y \frac{T_m^{p+1} - T_m^p}{\Delta t} \qquad (7)$$

$$T_m^{p+1} = \frac{\alpha \Delta t}{(\Delta z)^2}\left\{2\frac{h \Delta z}{k} T_\infty + 2T_{m-1}^p + \left[\frac{(\Delta z)^2}{\alpha \Delta t} - 2\frac{h \Delta z}{k} - 2\right] T_m^p\right\} \qquad (8)$$

To ensure convergence in the numerical solution, all selections of the parameter $\frac{(\Delta z)^2}{\alpha \Delta t}$ must be restricted according to

$$\frac{(\Delta z)^2}{\alpha \Delta t} \geq 2\left(\frac{h \Delta z}{k} - 1\right)$$

In terms of resistance – capacity formulation (6) and (8) takes the form:

$$T_i^{p+1} = \frac{\Delta t}{C_i}\left[q_i + \sum_j \frac{T_j^p - T_i^p}{R_{ij}}\right] + T_i^p \qquad (9)$$

Where $C_i = \rho_i c_i \Delta V_i$

And $q_i = 0$ for no heat generation

$R_{m+} = R_{m-} = \frac{\Delta z}{kA}$ inside the composite

$R_\infty = \frac{1}{hA}$ at the surface of the laminate

Table 1. Properties of air at atmospheric pressure

T, K	ϱ kg/m³	c_p kJ/kg.K	μ x10⁵, kg/m.s	ν x10⁶ m²/s	k w/m.K	α x10⁴ m²/s	Pr
100	3.6010	1.0266	0.6924	1.923	0.009246	0.02501	0.770
150	2.3675	1.0099	1.0283	4.343	0.013735	0.05745	0.753
200	1.7684	1.0061	1.3289	7.490	0.01809	0.10165	0.739
250	1.4128	1.0053	1.5990	11.31	0.02227	0.15675	0.722
300	1.1774	1.0057	1.8462	15.69	0.02624	0.22160	0.708
323	1.0949	1.0072	1.9514	18.02	0.02798	0.2569	0.703
350	0.9980	1.0090	2.075	20.76	0.03003	0.2983	0.697
400	0.8826	1.0140	2.286	25.90	0.03365	0.3760	0.689
450	0.7833	1.0207	2.484	31.71	0.03707	0.4222	0.683
500	0.7048	1.0295	2.671	37.90	0.04038	0.5564	0.680

Curled from (Holman, 2001)

ISSN 2319–7757 EISSN 2319–7765 | OPEN ACCESS

The air properties change with pressure and temperature. At atmospheric pressure, the air properties vary with temperature as in Table 1 and visually presented in Fig. 3 for trend observation. The desired properties of air at 323 K is obtained through interpolation.

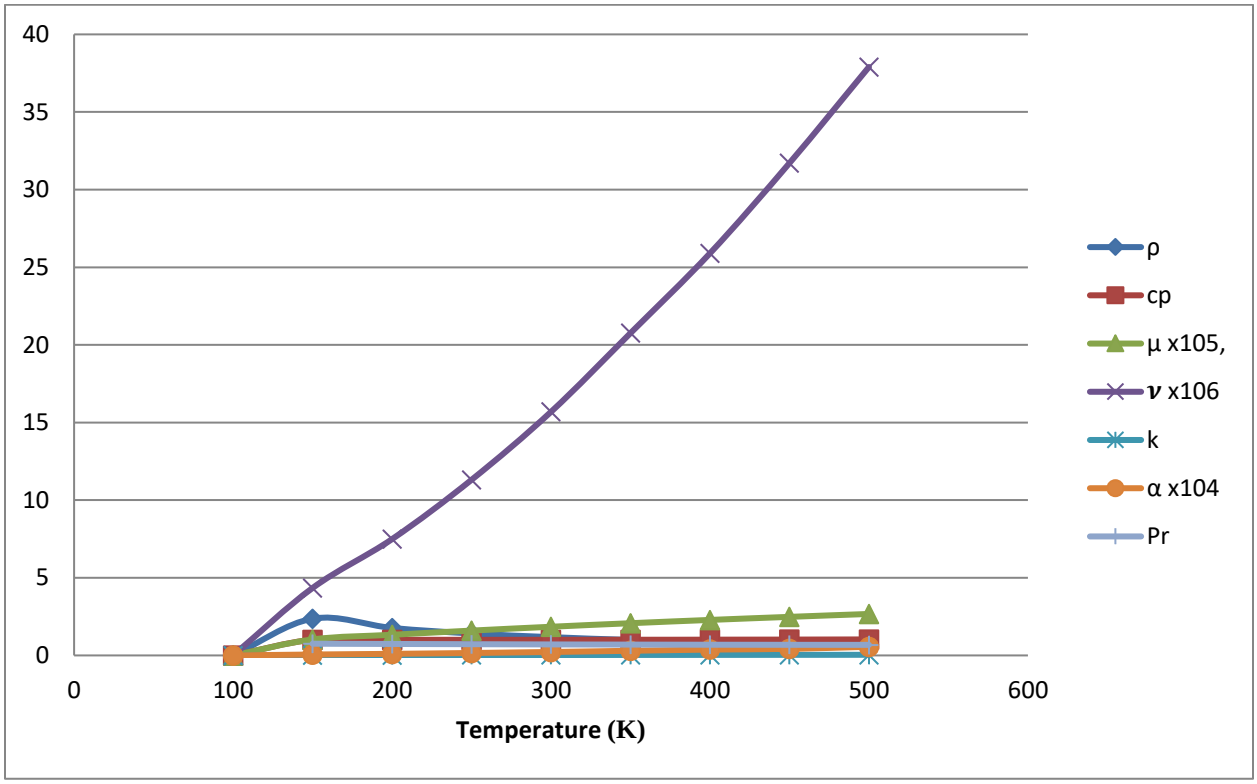

Figure 3. Variation of air properties with temperature, (K)

The applications of equation (9) to laminates of usual thicknesses of between 3 mm and 10 mm as obtained within the auto industry will provide a good evaluation that may lead to general inferences. In the cases of laminate thicknesses of 3mm and 10 mm the temperature distribution across the thickness can be visualized from the following analysis shown in Tables 2, 3 and 4. The values in Table 2 is applied to determine the time increment appropriate for the calculations of the temperature distribution which is obtained as 3 secs. For the 3 mm thick laminate 4 nodes were chosen (see Table 3) while for 10 mm thick laminate, 11 nodes were chosen (see Table 4).

Table 2. The determination of appropriate time increment for the 10 mm thick laminate

Node	$\sum(1/R_{ij})$	C_i	$\frac{C_i}{\sum(1/R_{ij})}$, s
1	208.912	627.48	3.00356131
2	404	1254.96	3.10633663
3	404	1254.96	3.10633663
4	404	1254.96	3.10633663
5	404	1254.96	3.10633663
6	404	1254.96	3.10633663
7	404	1254.96	3.10633663
8	404	1254.96	3.10633663
9	404	1254.96	3.10633663
10	404	1254.96	3.10633663
11	205.456	627.48	3.05408457

ISSN 2319–7757 EISSN 2319–7765 I OPEN ACCESS

Table 3. Numerical computations for the 3-ply 3 mm thickness laminate

No. of time increment (Δt =3 sec).	T_1	T_2	T_3	T_4
0	70	70	70	70
1	68.6781	70.0000	70.0000	69.3391
2	68.6766	69.3617	69.6808	69.3274
3	68.0601	69.1850	69.3560	69.0189
4	67.8887	68.7244	69.1107	68.6998
5	67.4437	68.5074	68.7257	68.4571
6	67.2336	68.0992	68.4906	68.0811
7	66.8391	67.8702	68.1039	67.8474
8	66.6175	67.4851	67.8672	67.4697
9	66.2454	67.2506	67.4908	67.2344
10	66.0185	66.8812	67.2510	66.8668
100	47.2539	47.6987	47.8459	47.6920
200	37.6239	37.8206	37.8855	37.8176
500	30.6577	30.6747	30.6803	30.6745
1000	30.0111	30.0114	30.0115	30.0114
1200	30.0022	30.0022	30.0022	30.0022

Table 4. Numerical computations for the 10-ply 10 mm thick laminate

No. of time increment (Δt =3 sec).	T_1	T_2	T_3	T_4	T_5	T_6	T_7	T_8	T_9	T_{10}	T_{11}
0	70.00	70.00	70.00	70.00	70.00	70.00	70.00	70.00	70.00	70.00	70.00
1	68.68	70.00	70.00	70.00	70.00	70.00	70.00	70.00	70.00	70.00	69.34
2	68.68	69.36	70.00	70.00	70.00	70.00	70.00	70.00	70.00	69.68	69.33
3	68.06	69.34	69.69	70.00	70.00	70.00	70.00	70.00	69.85	69.66	69.02
4	68.04	68.89	69.67	69.85	70.00	70.00	70.00	69.93	69.83	69.44	69.00
5	67.61	68.86	69.38	69.84	69.93	70.00	69.96	69.92	69.69	69.42	68.78
6	67.57	68.51	69.35	69.66	69.92	69.95	69.96	69.83	69.67	69.24	68.75
7	67.23	68.46	69.09	69.63	69.81	69.94	69.89	69.81	69.54	69.21	68.58
8	67.19	68.17	69.05	69.46	69.79	69.85	69.88	69.72	69.51	69.07	68.55
9	66.91	68.12	68.82	69.42	69.66	69.83	69.79	69.70	69.40	69.03	68.41
10	66.86	67.88	68.77	69.25	69.63	69.73	69.76	69.60	69.37	68.91	68.38
100	59.13	60.06	60.84	61.46	61.94	62.26	62.42	62.43	62.28	61.97	61.51
200	53.03	53.76	54.37	54.87	55.25	55.50	55.63	55.64	55.52	55.28	54.91
500	41.38	41.74	42.04	42.29	42.48	42.60	42.67	42.67	42.61	42.49	42.31
1000	33.51	33.63	33.72	33.80	33.85	33.89	33.91	33.91	33.90	33.86	33.80
2000	30.34	30.35	30.35	30.36	30.37	30.37	30.37	30.37	30.37	30.37	30.36
3000	30.03	30.03	30.03	30.03	30.04	30.04	30.04	30.04	30.04	30.04	30.03
3600	30.01	30.01	30.01	30.01	30.01	30.01	30.01	30.01	30.01	30.01	30.01
4000	30.00	30.00	30.00	30.00	30.00	30.00	30.00	30.00	30.00	30.00	30.00

ISSN 2319–7757 EISSN 2319–7765 I OPEN ACCESS

2. EXPERIMENT VALIDATION

2.1. Materials

E-glass chopped strand mat obtained as a continuous flat sheet serves to reinforce the polymer matrix. The fibres are evenly and randomly distributed and are held together in a powdered binder to obtain a mat area density of 450 g/m^2. It is quasi-isotropic in the in-plane directions. The polymer matrix is of the ortho-phthalic unsaturated polyester resin composition. The catalyst used is methyl ethyl ketone peroxide, while the cobalt derivative served as the accelerator. Galvanized mild steel plate mould; oven; remote thermometer; scissors; brushes; knife; bowels; stirrer; metering syringes are part of the tools employed for the experiment.

2.2. Methods

The wet lay-up method was adopted during the laminate samples fabrication to ensure close monitoring and simplicity. Four pieces of mild steel sheets of 350mm x 220mm x 2mm were cut from a mild steel sheet and served as a mould. The laminate was prepared in two sizes, one has three plies of 320 X 150 mm and another has ten plies of 100 x 80 mm. The probe of a remote thermometer was securely attached to the laminate surface to monitor the curing temperature. Readings were obtained as the temperature rises during cure and falls after cure. The laminate was removed from mould 24 hrs later to avoid springing and bending that could arise if removed immediately after hardening. Three moulds of neat resin were also cured at different temperature regimes to appreciate its effects.

3. RESULTS AND DISCUSSION

From preliminary investigation, the maximum exothermic temperature reached by the laminate is 70℃ at which cure takes place and also regarded as the free thermal stress state. The residual stresses are generated upon cooling to the ambient or storage temperature of 30℃

Hence the film temperature $T_f = \frac{70+30}{2} = 50℃ = 323K$

The air properties at 323K were obtained by linear interpolation as shown in Table 1, therefore:

$$Ra = GrPr = \frac{(9.8)(0.003096)(70-30)(.06)^3}{(18.02\times10^{-6})^2}(0.703) = 567526.992 \approx 5.68\times10^5$$

Hence equations (1) and (2) applies

$$Nu = 0.54(Ra)^{1/4} = 0.54(567526.992)^{1/4} = 14.8214$$

$$Nu = \frac{hL}{k}$$

$$h_{top} = \frac{Nu(k)}{L} = \frac{14.8214(0.02798)}{0.06} = 6.912W/m^2\,℃$$

$$Nu = 0.27(Ra)^{1/4} = 0.27(567526.992)^{1/4} = 7.4107$$

$$h_{bottom} = \frac{7.4107(0.02798)}{0.06} = 3.456W/m^2℃$$

The condition for lumped capacity thermal analysis:

Biot number $Bi = \frac{hs}{k} < 0.1$

$h_{average}$ = (6.912 + 3.456)/2 = 5.184W/m^2^{o}C

for a laminate 3mm thick

ISSN 2319–7757 EISSN 2319–7765 I OPEN ACCESS

$$Bi = \frac{6.912 \times 0.0015}{0.2020} = 0.05 < 0.1$$

The result indicates that for a 3 mm thickness laminate lumped capacity can be comfortably applied as the Biot number obtained is below the 0.1 critical value.

For a thickness of 10mm

$$Bi = \frac{6.912 \times 0.005}{0.2020} = 0.17 > 0.1$$

The result from 10 mm thick laminate is however above the specified critical value. Nonetheless, the difference is not large enough to distort the prediction arbitrarily, also, considering a more liberal condition that if

$$\frac{2k}{ht} > 6$$

lumped heat capacity analysis yields reasonable estimates.

Thus, for all $t < \frac{2k}{6h}$ $ie(\frac{2\times0.2020}{6\times6.912} = 0.00974 = 9.74mm \approx 10mm)$ lumped-capacity analysis applies. The value determined from the second criterion is approximately 10 mm justifying the adoption of the lumped capacity assumption as well.

Figures 4 and 5 show the change in temperature with time on the laminate surface with 3 mm and 10 mm thicknesses respectively as obtained through numerical analysis and by experimental measurements. It was observed that the numerical computation under-predicted the temperatures just after the commencement of the cooling process in the 3 mm thickness laminate while over-predicted the temperatures in the 10 mm thickness laminates. This may be due partly to the effect of edge losses predominant in thick materials unaccounted for in the thicker laminate analysis. Also, the abrupt changes in environmental factors idealized in the numerical method may have contributed to the discrepancy observed. The error is less in the 3 mm thickness laminate with 15% maximum as opposed to about 28% in the 10 mm thickness laminate. This suggests that lumped parameter analysis gives better estimates with thin laminates.

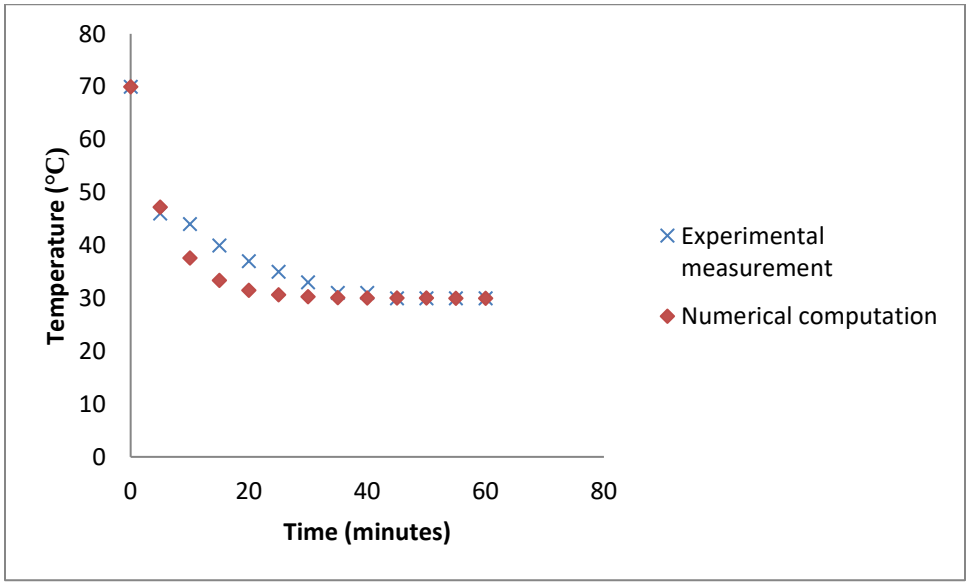

Figure 4. Cool-down temperature versus time for the 3-ply 3 mm thickness laminate

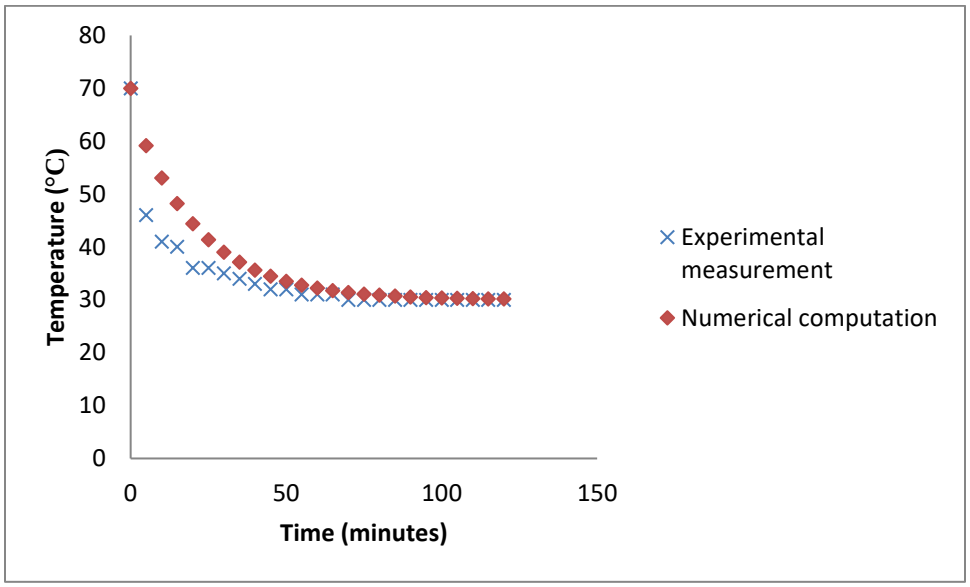

Figure 5. Cool-down temperature versus time for a 10-ply 10 mm thickness laminate

Figure 6 visualizes the temperature distribution across the thickness through the 10 mm thick laminate after 300 seconds of cooling down. The trend was determined from the values obtained through numerical computations. It was found that a preponderance exists in the temperature peak location towards the steel mould. This may be because heat loss from the top is more when compared to the heat loss through the bottom.

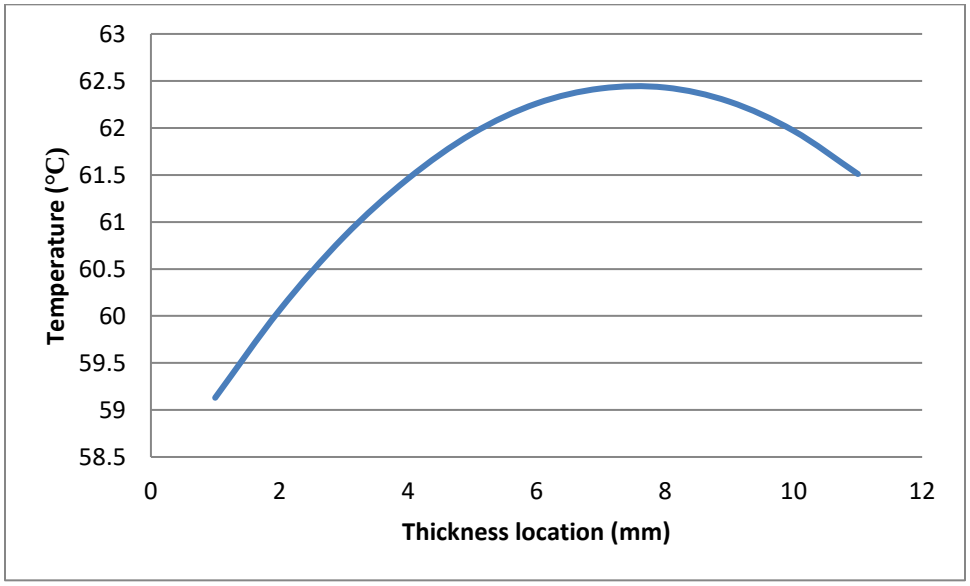

Figure 6. Temperature profile across the 10-ply 10 mm thick laminate after 300 seconds.

The associated biaxial stress in the laminate surface due to temperature gradient across the thickness is then obtained as follows (Hyer, 1998).

$$\sigma_1^T = \sigma_2^T = \sigma^T = \left(\frac{1}{1-\nu^2} + \frac{\nu}{1-\nu^2}\right) E\alpha\Delta T$$

$$= \left(\frac{1+\nu}{(1-\nu)(1+\nu)}\right) E\alpha\Delta T$$

$$= \frac{1}{1-\nu} E\alpha\Delta T$$

$$\sigma_1^T = \sigma_2^T = \sigma^T = \frac{1}{1-\nu} E\alpha\Delta T \qquad (10)$$

Equation (10) gives the residual thermal stress within the composite as it cools from the high cure temperature down to ambient.

where E is Young's modulus, α = the linear coefficient of thermal expansion, ΔT is the temperature gradient and ν is the Poisson's ratio. For E = 8 GPa, ν= 0.4, $\alpha = 30 \times 10^{-6}$m/m/K. Considering the temperature distribution shown in Fig. 6 with a maximum change in temperature of 3.3 °C across the thickness from the core at node 8, and the surface at node 1. The maximum residual thermal stress due to temperature gradient is obtained as 1.32MPa.

The major effect of uncontrolled temperature gradient in laminated composites is the residual stresses development which may lead to cracks and failure of the component even before been used. For an illustration, the cooled neat resin cured with cracks is depicted in Fig. 7. It is observed that as the temperature gradient increases the larger the cracks developed indicating higher residual stress accumulation.

Figure. 7 A sample of cracking effect of cure temperature on neat resin mouldings.

4. CONCLUSION

It is established that the lumped parameter analysis subsists if the random fibre laminate thickness, the conductivity and the convective heat transfer are coupled within the Biot parameter and criterion. The spatial temperature distribution in the fibre mat reinforced laminate, therefore, can be considered under a thin plate with lumped parameter analysis if the thickness is below 10 mm. For the fact that appreciable quantity of composite parts produced for the automotive industry fall within the thicknesses of consideration, 3 – 10 mm (which is from 3 to 10 plies of 450g/m² glass fibre) it is sufficient therefore to apply the lumped-capacity analysis. An important remark though is the fact concerning the cooling and convective heat transfer input values and observations which were determined under a natural convective environment. This is so because most laminations using the wet hand layup method as prevalent in the automotive industries are cured under a natural environment.

Funding:
This study has not received any external funding.

Conflict of Interest:
The authors declare that there are no conflicts of interests.

Data and materials availability
All data associated with this study are present in the paper.

ISSN 2319–7757 EISSN 2319–7765 | OPEN ACCESS

REFERENCES AND NOTES

1. Agbo, Cornelius O. A., Boniface A. Okorie and Daniel O. N. Obikwelu. Control of stress relaxation and residual thermal stress during cure of random fibre mat-reinforced polyester composites. Journal of Composite Materials, 2017, Vol. 51(22) 3127–3136
2. An, Chen and Jian Su. Lumped models for transient thermal analysis of multi-layered composite pipeline with active heating. Applied Thermal Engineering, 87 (2015) 749e759
3. Antonucci, Vincenza, Cusano A., Giordano Michele, Nasser J., Nicolais Luigi. Cure-Induced Residual Strain Build-up in a Thermoset Resin, Composites Part A; Applied Science and Manufacturing, 37(4), 2006. pp 592 – 601.
4. Cao, Zhongliang, Mingjun Dong, Kailei Liu and Hongya Fu. Temperature Field in the Heat Transfer Process of PEEK Thermoplastic Composite Fiber Placement. Materials 2020, 13, 4417; doi:10.3390/ma13194417
5. Christensen, R. M. Theory of Viscoelasticity (2nd ed.), Dover Pub, Mineola, New York, 1982.
6. Dieter, G. E. Mechanical Metallurgy, McGraw-Hill, London, 1988.
7. Holman, J. P. Heat Transfer (8th ed), Tata McGraw-Hill, New Delhi, 2001.
8. Hyer, M. W. Stress Analysis of Fiber-Reinforced Composite Materials, WCB/McGraw-Hill, Boston, USA, 1998.
9. Kibler, K. G. Time Dependent Environmental Behaviour of Graphite/Epoxy Composites, Air Force Wright Aeronautical Laboratories (AFWAL-TR-80-4052), Ohio, 1980.
10. Lee, K. and Y. Weitsman, Optimal Cool Down in Nonlinear Thermoviscoelasticity with Application to Graphite / Peek (APC-2) Laminates, ASME, Journal of Applied Mechanics, vol. 61, pp 367 – 374. 1994.
11. Li, Xiangqian, Stephen R. Hallett, Michael R. Wisnom. A finite element based statistical model for progressive tensile fibre failure in composite laminates. Composites Part B: Engineering, 45(1) 2013 433-439.
12. Sonmez, F. O. and Erhan Eyol, Optimal Post-Manufacturing Cooling Paths for Thermoplastic Composites, Composites Part A: Applied Science and Manufacturing, vol. 33, pp. 301 – 314, 2002.
13. Tegenaw, Petros Demissie, Mekonnen Gebreslasie Gebrehiwot, Maarten Vanierschot. On the comparison between Computational Fluid Dynamics (CFD) and lumped capacitance modelling for the simulation of transient heat transfer in solar dryers. Solar Energy · May 2019. DOI: 10.1016/j.solener.2019.04.024
14. Weitsman, Y. Residual Thermal Stresses Due to Cool-Down of Epoxy-Resin Composites, ASME, Journal of Applied Mechanics, vol. 46, pp. 563 – 567, 1979.

ISSN 2319–7757 EISSN 2319–7765 | OPEN ACCESS